

RESEARCH

Open Access



The additional value of ^{18}F -FDG PET/CT imaging in guiding the treatment strategy of non-tuberculous mycobacterial patients

Donghe Chen¹, Yunbo Chen², Shuye Yang¹, Kanfeng Liu¹, Zhen Wang¹, Tingting Zhang¹, Guolin Wang¹, Kui Zhao^{1*} and Xinhui Su^{1*}

Abstract

Objectives Non-tuberculous mycobacteria (NTM) infection is an increasing health problem due to delaying an effective treatment. However, there are few data on ^{18}F -FDG PET/CT for evaluating the status of NTM patients. The aim of this study was to investigate the potential value of ^{18}F -FDG PET/CT in guiding the treatment strategy of NTM patients.

Methods We retrospectively analyzed the cases of 23 NTM patients who underwent ^{18}F -FDG PET/CT. The clinical data, including immune status and severity of NTM pulmonary disease (NTM-PD), were reviewed. The metabolic parameters of ^{18}F -FDG included maximum standardized uptake value (SUV_{max}), SUV_{max} of the most FDG-avid lesion (SUV_{Top}), $\text{SUV}_{\text{Top}}/\text{SUV}_{\text{max}}$ of the liver ($\text{SUR}_{\text{Liver}}$), $\text{SUV}_{\text{Top}}/\text{SUV}_{\text{max}}$ of the blood ($\text{SUR}_{\text{Blood}}$), metabolic lesion volume (MLV), and total lesion glycolysis (TLG). The optimal cut-off values of these parameters were determined using receiver operating characteristic curves.

Results There were 6 patients (26.09%) with localized pulmonary diseases and 17 patients (73.91%) with disseminated diseases. The NTM lesions had high or moderate ^{18}F -FDG uptake (median SUV_{Top} : 8.2 ± 5.7). As for immune status, the median SUV_{Top} in immunocompromised and immunocompetent patients were 5.2 ± 2.5 and 10.0 ± 6.4 , respectively, with a significant difference ($P = 0.038$). As for extent of lesion involvement, $\text{SUR}_{\text{Liver}}$ and $\text{SUR}_{\text{Blood}}$ in localized pulmonary and disseminated diseases were 1.9 ± 1.1 vs. 3.8 ± 1.6 , and 2.7 ± 1.8 vs. 5.5 ± 2.6 , respectively, with a significant difference ($P = 0.016$ and 0.026). Moreover, for disease severity, SUV_{max} of the lung lesion (SUV_{Lung}) and SUV_{max} of the marrow ($\text{SUV}_{\text{Marrow}}$) in the severe group were 7.7 ± 4.3 and 4.4 ± 2.7 , respectively, significantly higher than those in the non-severe group (4.4 ± 2.0 and 2.4 ± 0.8 , respectively) ($P = 0.027$ and 0.036). The ROC curves showed that SUV_{Top} , $\text{SUR}_{\text{Liver}}$, $\text{SUR}_{\text{Blood}}$, SUV_{Lung} , and $\text{SUV}_{\text{Marrow}}$ had a high sensitivity and specificity for the identification of immune status, lesion extent, and severity of disease in NTM patients.

Conclusion ^{18}F -FDG PET/CT is a useful tool in the diagnosis, evaluation of disease activity, immune status, and extent of lesion involvement in NTM patients, and can contribute to planning the appropriate treatment for NTM.

*Correspondence:

Kui Zhao
zhaokui0905@zju.edu.cn
Xinhui Su
suxinhui@zju.edu.cn

Full list of author information is available at the end of the article



© The Author(s) 2024. **Open Access** This article is licensed under a Creative Commons Attribution 4.0 International License, which permits use, sharing, adaptation, distribution and reproduction in any medium or format, as long as you give appropriate credit to the original author(s) and the source, provide a link to the Creative Commons licence, and indicate if changes were made. The images or other third party material in this article are included in the article's Creative Commons licence, unless indicated otherwise in a credit line to the material. If material is not included in the article's Creative Commons licence and your intended use is not permitted by statutory regulation or exceeds the permitted use, you will need to obtain permission directly from the copyright holder. To view a copy of this licence, visit <http://creativecommons.org/licenses/by/4.0/>. The Creative Commons Public Domain Dedication waiver (<http://creativecommons.org/publicdomain/zero/1.0/>) applies to the data made available in this article, unless otherwise stated in a credit line to the data.

Keywords Non-tuberculous mycobacteria, NTM-PD, Disseminated NTM infection PET/CT, ^{18}F -FDG

Introduction

Non-tuberculous mycobacteria (NTM) are *Mycobacterium* (*M.*) species other than *M. leprae* and *M. tuberculosis*. NTM are prevalent in the environment, such as soil, dust, plants, water sources, foods, and animals, and are more likely to infect immunocompromised than immunocompetent individuals [1]. The prevalence of diseases caused by NTM has increased in recent years; for instance, in the United States, the number of people affected rose from 40 to 85 per 100,000 individuals between 2010 and 2014 [2]. In China, NTM-related diseases have also gradually become more common over the last 20 years [3], with more than 170 NTM species reported [4, 5].

NTM can cause a variety of clinical syndromes ranging from lymphadenopathy to aseptic meningitis [6, 7]. The most common clinical manifestation of NTM infection is NTM pulmonary disease (NTM-PD). Furthermore, extra-pulmonary NTM diseases, such as infections of soft tissues, lymph nodes or bone, can emerge as a result of NTM exposure [5]. The primary diagnostic methods are culture of clinical samples, and molecular and genetic detection (including DNA PCR assay, metagenomic next-generation sequencing (mNGS) from body fluid or histopathological tissue) [9]. However, these methods are invasive, requiring biopsies from patients. In addition, the sensitivity and accuracy of these procedures are limited due to sampling errors or contamination, as well as NTM heterogeneity within biopsy samples [8, 9].

Computed tomography (CT) has been widely used in the diagnosis of pulmonary diseases. However, NTM-PD have poor specific radiological manifestations. NTM can also infect organs and tissues besides lungs, such as the skin, bones and soft tissues, also known as disseminated NTM infections due to immune status [5]. The current guidelines for NMT treatment, such as the Official ATS/ERS/JRS/ALAT Clinical Practice Guideline for Treatment of NTM in 2020 [10] and the British Thoracic Society guidelines for the management of NTM pulmonary disease in 2017 [11], strongly recommend that individuals may require a period of longitudinal assessment (including immune status, the severity and risk of progressive NTM infection, and the extent of lesion involvement) before a decision is made to start treatment. Therefore, it is critical to develop a noninvasive imaging tool for evaluating active lesion, immune status, and the extent of lesion involvement [12].

^{18}F -FDG (2- ^{18}F -fluoro-2-deoxy-D-glucose) is a non-physiological glucose analogue, which is metabolized by the same physiological processes as glucose [13]. Inflammatory cells with multiple mechanistic similarities to

malignant cells, such as macrophages, demonstrate greater FDG uptake [13]. ^{18}F -FDG PET/CT has been used for detecting inflammation and infection such as fever of unknown origin (FUO), sarcoidosis, IgG4-related systemic disease, and human immunodeficiency virus (HIV)-related infections, among others. Its roles in diagnosis include mapping extent of disease, assessing therapy response based on whole-body imaging, and changes in FDG metabolic parameters ahead of morphological changes by conventional imaging techniques (CT and MRI) [14–16]. Moreover, ^{18}F -FDG PET/CT has been suggested as a potential tool for evaluating the responsiveness of tuberculosis (TB) infection to anti-tuberculosis therapy [17, 18]. A few case reports have indicated a possible value of ^{18}F -FDG PET/CT for patients with NTM [19–22]. However, available data concerning the findings of ^{18}F -FDG PET/CT in NTM has been limited. Furthermore, according to the guidelines for the management of non-tuberculosis mycobacterial pulmonary disease by the British Thoracic Society [11], the choice of therapeutic strategy relies strongly on the immune status, extent of lesion involvement, and disease severity in NTM patients. Meanwhile, there are limited data on the use of ^{18}F -FDG PET/CT for evaluating the status of NTM patients. Therefore, this retrospective study was performed to investigate and confirm the potential value of ^{18}F -FDG PET/CT in guiding the treatment strategy in NTM patients.

Materials and methods

Patient information

We retrospectively reviewed 23 patients with a confirmed diagnosis of NTM infection who underwent ^{18}F -FDG PET/CT between December 2016 and October 2021 in the First Affiliated Hospital, Zhejiang University School of Medicine. The flow diagram of the study design is presented in Fig. 1. The clinical information (age, gender, risk factor, and syndrome) and laboratory test results (serum cytokines, immune cell, and mycobacterium species) were obtained by reviewing the available medical records. A total of 16 patients underwent ^{18}F -FDG PET/CT imaging before anti-NTM therapy, while the other 7 patients underwent ^{18}F -FDG PET/CT imaging after anti-NTM treatment (within less than 6 months).

Based on the risk factors of immune status, the 23 enrolled patients were divided into two groups: immunocompromised patients and immunocompetent patients. According to a previous article [23], immunocompromised patients were defined as follows: those with primary immune deficiency disease; active malignancy; receiving cancer chemotherapy; HIV infection with a

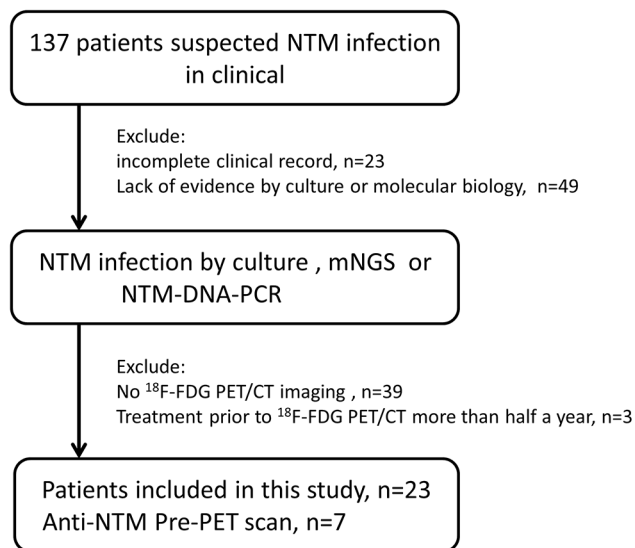


Fig. 1 Flow diagram showing the patient selection details. NTM: Non-tuberculous mycobacteria; ^{18}F -FDG PET/CT: ^{18}F -fluorodeoxyglucose positron emission tomography/computed tomography; mNGS: Metagenomic next-generation sequencing; NTM-DNA-PCR: PCR assay for non-tuberculous mycobacterial DNA

CD4 T-lymphocyte count < 200 cells/mL; solid organ transplantation; hematopoietic stem cell transplantation; receiving corticosteroid therapy with a dose 20 mg prednisone or equivalent daily for ≥ 14 days or a cumulative dose > 700 mg of prednisone; receiving biologic immune modulators (such as azathioprine, corticosteroids and mesalazine etc.); receiving disease-modifying anti-rheumatic or other immunosuppressive drugs. Based on the extent of lesion involvement in NTM patients [24, 25], these 23 patients classified into two groups: localized pulmonary diseases group and disseminated diseases group. The patients with NTM disease involvement only in lungs were defined as localized pulmonary diseases, while the patients with NTM disease involvement both in lungs and other tissues or organs (such as skin, lymph nodes, bone and joint, soft tissue, urinary system, etc.) were defined as disseminated diseases. According to the disease severity, these patients were further classified into severe and non-severe disease groups based on the British Thoracic Society guidelines for the management of NTM-PD in 2017 [5, 11]. Non-severe disease included: (a) mild-moderate symptoms, (b) no signs of systemic illness, (c) absence of lung cavitation and extensive lung disease, (d) acid-fast bacilli (AFB) smear-negative in the pulmonary specimens. Severe disease included: (a) presence of severe symptoms and signs of systemic illness, (b) presence of lung cavitation and extensive lung involvement, (c) pulmonary specimens positive for acid-fast bacilli (AFB) smear.

^{18}F -FDG PET/CT imaging

^{18}F -FDG was synthesized using a Siemens Eclipse cyclotron (Siemens Medical Solutions, Knoxville, TN 37,932, USA) and a Siemens Explora FDG4 chemical synthesis module. The patients were fasted for at least 4 h before being injected with ^{18}F -FDG at a dose of 4.44 to 5.55 MBq/kg. Images were acquired using a PET/CT instrument (Biograph 16 and Version, Siemens Company, Germany). Two experienced nuclear medicine physicians independently reviewed PET/CT images until consensus was reached. Semiquantitative analysis was performed using the maximum standardized uptake value (SUV_{max}). Furthermore, 10 metabolic parameters were also recorded: SUV_{Top} (SUV_{max} of the most FDG-avid lesion), $\text{SUV}_{\text{I-Lung}}$ (SUV_{max} of intra-pulmonary lesions), $\text{SUV}_{\text{E-Lung}}$ (SUV_{max} of extra-pulmonary lesions), $\text{SUV}_{\text{Liver}}$ (SUV_{max} of the liver), $\text{SUV}_{\text{Spleen}}$ (SUV_{max} of the spleen), $\text{SUV}_{\text{Marrow}}$ (SUV_{max} of the marrow), $\text{SUR}_{\text{Liver}}$ (the most FDG-avid lesion-to-liver SUV_{max} ratio) and $\text{SUR}_{\text{Blood}}$ (the most FDG-avid lesion-to-blood pool SUV_{max} ratio), metabolic lesion volume (MLV) and total lesion glycolysis (TLG). The MLV of each lesion was calculated using an automated region-growing algorithm with SUV thresholds of 2.5. The TLG was measured as MTV multiplied by the average SUV of each lesion.

Statistical analysis

Quantitative data were presented as mean and standard deviation. All statistical analyses were performed using GraphPad Prism, version 8.0 (GraphPad Software, San Diego, CA, USA). The differences in immune status, extent of lesion involvement and severity of NTM-PD were analyzed using the chi-squared test. A p -value of less than 0.05 was considered statistically significant. ROC curves were used to determine the optimal cut-off values.

Results

Patients' clinical characteristics

The demographics and clinical features of the 23 patients with NTM infection were summarized in Table 1. These patients included 19 (82.6%) men and 4 (17.4%) women, with an age range between 14 and 84 years (median, 60.0 years). The diagnosis of these patients was confirmed by tissue culture ($n=6$), non-tuberculous mycobacteria DNA PCR assay (NTM-DNA-PCR) ($n=3$), and metagenomic next-generation sequencing (mNGS) ($n=14$). Specimens were collected from blood or bronchoalveolar lavage fluid (BALF), pus, sputum, tissue of lung lesions, and bone lesions. The most frequent NTM species detected was *M. intracellulare* (12 cases, 52.1%), and 1 patient had mixed infection with *M. intracellulare* and *M. kansasii*.

Table 1 Demographics and clinical characteristics of patients with NTM infection

No.	Gender	Age	Bacterial species	Risk factor	Clinical symptoms	Diagnosis	Involved sites	Anti-NTM Pre-PET scan	SUV _{Top}	MLV	TLG	PET/CT findings
1	M	38	<i>M. abscessus</i>	COPD	Fever, cough	mNGS (BALF)	Bilateral lungs	None	11.3	161.3	578.8	Pulmonitis
2	M	58	<i>M. intracellulare</i>	COPD	Ostealgia	Culture (Pus)	Right lung, multiple bones	None	14.8	438.8	1802.5	MM
3	M	71	<i>M. intracellulare</i>	Pulmonary TB history	Fatigue, cough	TB-DNA-PCR (Sputum)	Bilateral lungs, lymph nodes, adrenals	None	11.8	972.6	4628.6	Pulmonitis
4	M	84	<i>M. intracellulare</i>	COPD	Cough	Culture (Blood)	Bilateral lungs, lymph nodes	Oral of 1 weeks	7.5	42.6	148.7	Pulmonitis
5	M	29	<i>M. abscessus</i>	AIDS	Fever	Culture (lymph node)	Bilateral lungs, lymph nodes	Oral Azi + Eth + Rif 3 months	6.6	48.2	128.4	Lymphadenoma
6	M	79	<i>M. intracellulare</i>	COPD	Chest tightness	mNGS (BALF)	Left lung, lymph nodes	None	4.1	27.3	79.7	Pulmonitis
7	M	50	<i>M. chimaera</i>	Chemotherapy of lymphoma	None	mNGS (BALF)	Bilateral lungs	None	2.4	0	0	Pulmonitis
8	M	61	<i>M. intracellulare</i>	Splenectomy	Ostealgia	mNGS (bone surgery)	Multiple bones, lymph nodes	None	6.0	58	200.3	MM
9	M	44	<i>M. kansasii</i>	None	Ostealgia	mNGS (bone biopsy)	Bilateral lungs, lymph nodes, multiple bones, subcutaneous	None	28.1	129.9	637.7	Lung cancer and multiple metastases
10	F	60	<i>M. abscessus</i>	Chemotherapy of leukemia	None	TB-DNA-PCR (Sputum)	Bilateral lungs	Oral Azi + Eth + Rif 5 months	1.2	0	0	Pulmonitis
11	F	14	<i>M. Avium</i>	MonoMAC syndrome	Fever, cough	mNGS (lung puncture)	Bilateral lungs, lymph nodes	None	5.1	70.9	244.1	Pulmonitis
12	M	63	<i>M. intracellulare</i>	History of lung cancer	Ostealgia	mNGS (bone biopsy)	Bilateral lungs, lymph nodes, multiple bones	None	7.9	137.6	539.1	Bone metastases
13	M	19	<i>M. Avium</i>	Hepatitis B cirrhosis	Fever	TB-DNA-PCR (Sputum)	Right lung, lymph nodes	Oral Eth + Rif 1 weeks	5.5	60.3	211.2	Pulmonitis
14	M	60	<i>M. paraintracellulare</i>	Chemotherapy of lung cancer	cough	mNGS (BALF)	Bilateral lungs, left 7 rib	Oral Azi + Eth + Rif 2 months	4.5	27.8	88.4	Recurrence of lung cancer
15	F	70	<i>M. intracellulare</i>	None	Fever, ostealgia	mNGS (lung puncture)	Left lung, multiple bones	None	13.8	31.7	221.7	Lung cancer and metastases
16	F	60	<i>M. intracellulare</i>	Splenectomy	Fever, cough	Culture (Sputum)	Bilateral lungs, lymph nodes	None	13.0	309.8	1283.5	Pulmonitis
17	M	78	<i>M. intracellulare</i> + <i>M. kansasii</i>	COPD	Weight loss	mNGS (BALF)	Left lung	Oral Azi + Eth + Rif 2 months	8.3	0.7	2.6	Pulmonitis
18	M	73	<i>M. Avium</i>	None	Fever, cough	mNGS (lung puncture)	Bilateral lungs, lymph nodes	None	5.8	44.9	137.9	Lung cancer and metastases
19	M	61	<i>M. intracellulare</i>	Chemotherapy of Lung MALToma	Fatigue	mNGS (BALF)	Bilateral lungs, lymph nodes	None	5.2	135.1	666.1	Recurrence of lung maltona
20	M	27	<i>M. Avium</i>	AIDS	Fever	Culture (Blood)	Bilateral lungs, lymph nodes, spleen	Oral Cla + Mox + Eth + Rif 3 months	6.4	21.5	176.2	Pulmonitis
21	M	66	<i>M. intracellulare</i>	COPD	Cough	Culture (Sputum)	Bilateral lungs	None	3.4	1.2	3.3	IIP

Table 1 (continued)

No.	Gender	Age	Bacterial species	Risk factor	Clinical symptoms	Diagnosis	Involved sites	Anti-NTM Pre-PET scan	SUV _{top}	MLV	TLG	PET/CT findings
22	M	61	<i>M. abscessus</i>	Chemotherapy of pancreatic cancer	Fever	mNGS (BALF)	Bilateral lungs	None	6.3	38	124.8	Pulmonitis
23	M	55	<i>M. intracellulare</i>	Chemotherapy of MDS	Fever	mNGS (BALF)	Bilateral lungs, lymph nodes	None	9.9	52.4	216	Invasion of tumor

COPD: Chronic obstructive pulmonary disease; TB: Tuberculosis; AIDS: Acquired immunodeficiency syndrome; mNGS: Metagenomic next-generation sequencing; BALF: Bronchoalveolar lavage fluid; TB-DNA-PCR: Mycobacterium tuberculosis DNA; NTM: Non-tuberculous mycobacterial; Ofi: Ofloxacin; Azi: Azithromycin; Eth: Ethambutol; Rif: Rifampicin; Cla: Clarithromycin; Mox: Moxalactam; MM: multiple myeloma; IIP: idiopathic interstitial pneumonia

In terms of the risk factors of immune status, among the 23 patients, 9 (39.1%) were immunocompromised, including during chemotherapy (6 cases, 26.1%), due to lymphoma (2 cases), leukemia (one case), MDS (one case), lung cancer (one case), pancreatic cancer (one case), acquired immune deficiency syndrome (AIDS) (2 cases, 8.7%), and monocytopenia and mycobacterial infection syndrome (MonoMAC syndrome) (1 case, 4.3%). The other 14 patients were immunocompetent, of which 5 patients (37.8%) presented with underlying diseases, such as splenectomy (2 case, 8.6%), hepatitis B cirrhosis (1 case, 4.3%), tuberculosis (1 case, 4.3%), and early-stage lung cancer (1 case, 4.3%). Six patients exhibited a mild chronic obstructive pulmonary disease (COPD) because of long-term smoking, whereas 3 patients had no risk factors or underlying diseases.

Laboratory characteristics

The laboratory characteristics of the 23 patients with NTM infection were presented in Supplementary Table 1. The median white cell count was $7.6 \times 10^9/L$ (range: $2.3\text{--}22.8 \times 10^9/L$), and 10 patients (43.5%) had leukocytosis (10 cases, 43.5%). The median platelet count was $226 \times 10^9/L$ (range: $85\text{--}492 \times 10^9/L$), and 8 patients (34.8%) had thrombocytosis. The majority of patients showed varying levels of increase in the C-reactive protein (CRP) (16 cases, 69.6%), erythrocyte sedimentation rate (ESR) (15 cases, 65.2%) and interleukin 6 (IL-6) level, (20 cases, 87%). The other laboratory test results were almost within the normal range, including procalcitonin (PCT), serum cytokines, and cellular immune function in the peripheral blood.

¹⁸F-FDG PET/CT imaging characteristics

The ¹⁸F-FDG PET/CT imaging characteristics of the 23 patients with NTM infection were summarized in Table 2.

Intra-pulmonary lesions

¹⁸F-FDG PET/CT revealed NTM-PD in 22 patients (95.6%) with lung involvement, including the involvement of a single lobe (5 cases) and two lobes (17 cases). Among these patients, the common CT feature was the presence of patchy infiltrate (18 cases, 81.8%) and bronchiectasis (8 cases, 36.4%). Lesions with high FDG-uptake ($SUV_{I-Lung} > 2.5$) were observed in 19 patients (Fig. 2A, blue arrows) and those with low FDG-uptake ($SUV_{I-Lung} \leq 2.5$) were observed in 3 patients (Fig. 2B, white arrows).

Extra-pulmonary lesions

Extra-pulmonary lesions with abnormally high ¹⁸F-FDG FDG uptake were found in 17 patients (73.8%). Among them, ¹⁸F-FDG PET/CT showed increased ¹⁸F-FDG accumulation in the lymph node (14 cases), bone (6

Table 2 imaging characteristic of ^{18}F -FDG PET/CT in patients with NTM infection

Imaging characteristic	n (range or %)
Intra-pulmonary FDG accumulation	22(95.7)
Single lobe	5(21.7)
Double lobe	17(73.9)
Morphological manifestations in the lung	
Patchy infiltration	18(81.8)
Nodular infiltration	3(13.6)
Bronchiectasis	8(36.4)
Cavitation	5(22.7)
Calcification	3(13.6)
Atelectasis	2(9.1)
Pleural effusion	4(18.2)
Extra-pulmonary FDG accumulation	17(73.9)
Lymph nodes	14(60.9)
Bone	6(26.1)
Subcutaneous	1(4.3)
Spleen	1(4.3)
Adrenal gland	1(4.3)
Extent of lesion involvement	
Pulmonary NTM group	6(26.1)
Disseminated NTM group	17(73.9)
Metabolic parameters	mean (range)
SUV_{Top}	8.2 ± 5.7 (1.2–28.1)
$\text{SUV}_{\text{I-lung}}$	6.6 ± 3.9 (1.2–13.9)
$\text{SUV}_{\text{E-lung}}$	6.3 ± 6.3 (1.8–28.1)
$\text{SUV}_{\text{Liver}}$	2.7 ± 0.6 (1.7–3.8)
$\text{SUV}_{\text{Marrow}}$	3.7 ± 2.0 (1.7–6.7)
$\text{SUV}_{\text{Spleen}}$	2.5 ± 0.9 (1.7–6.0)
$\text{SUR}_{\text{Liver}}$	3.7 ± 2.3 (0.5–7.6)
$\text{SUR}_{\text{Blood}}$	5.9 ± 3.9 (0.7–10.3)
MLV (cm^3)	122.2 ± 211.7 (0–972.6)
TLG ($\text{ml}^* \text{SUV}$)	526.9 ± 992.1 (0–4628.6)

^{18}F -FDG PET/CT: ^{18}F -fluorodeoxyglucose positron emission tomography/computed tomography; NTM: Non-tuberculous mycobacterial infection; SUV_{Top} : The most FDG-avid lesion in the whole body; $\text{SUV}_{\text{I-lung}}$: SUV_{max} of lung lesions, $\text{SUV}_{\text{E-lung}}$: SUV_{max} of extra-lung lesions; $\text{SUV}_{\text{Liver}}$: SUV_{max} of liver; $\text{SUV}_{\text{Spleen}}$: SUV_{max} of spleen; $\text{SUV}_{\text{Marrow}}$: SUV_{max} of marrow; $\text{SUR}_{\text{Liver}}$: SUV_{max} ratio of lesion-to-liver; $\text{SUR}_{\text{Blood}}$: SUV_{max} ratio of lesion-to-blood pool. MLV: the metabolic lesion volume; TLG: total lesion glycolysis

cases), subcutaneous tissue (1 case), the spleen (1 case), and adrenal gland (1 case). Lesions with high FDG-uptake ($\text{SUV}_{\text{E-Lung}} > 2.5$) were observed in 15 patients, and those with low FDG-uptake ($\text{SUV}_{\text{E-Lung}} \leq 2.5$) were observed in 2 patients.

Extent of lesion involvement

Disseminated NTM infection was observed in 17 patients using ^{18}F -FDG PET/CT. Among them, involvements of the common multi-system were found in the lung and lymph nodes (9 cases), and lung and bone (3 cases) (Fig. 3). Other multi-system involvements included lung, lymph node, bone and subcutaneous tissue (1 case), lung, lymph node and bone (1 case), lung, lymph node and spleen (1 case), lung, lymph node and adrenal gland (1

case), and lymph node and bone (1 case). Localized pulmonary NTM infection was identified in 6 patients.

Metabolic parameters

The median SUV_{Top} in 23 patients with lung involvement was 8.2 ± 5.7 (range: 1.2–28.1); the median $\text{SUV}_{\text{I-Lung}}$ in 22 patients with lung involvement was 6.6 ± 3.9 (range: 1.2–13.9); the median $\text{SUV}_{\text{E-Lung}}$ in 17 patients was 6.3 ± 6.3 (range: 1.8–28.1); the median $\text{SUV}_{\text{Liver}}$, $\text{SUV}_{\text{Marrow}}$ and $\text{SUV}_{\text{Spleen}}$ were 2.7 ± 0.6 (range: 1.7–3.8), 3.7 ± 2.0 (range: 1.7–6.7), and 2.5 ± 0.9 (range: 1.6–6.0), respectively; the median $\text{SUR}_{\text{Liver}}$ and $\text{SUR}_{\text{Blood}}$ were 3.7 ± 2.3 (range: 0.5–9.1) and 5.9 ± 3.9 (range: 0.6–16.4), respectively; the median MLV and TLG were 122.2 ± 211.7 (range: 0–972.6) and 526.9 ± 992.1 (range: 0–4628.6), respectively.

^{18}F -FDG PET/CT characteristics in different immune states, extent of lesion involvement, and severity of NTM-PD

The comparison of clinical and ^{18}F -FDG PET/CT characteristics in patients with different immune states, extent of lesion involvement, and severity of NTM-PD were shown in Table 3; Fig. 4. As for the immune state, SUV_{Top} in immunocompetent patients was significantly higher than that in immunocompromised patients (median SUV_{Top} , 10.0 ± 6.4 vs. 5.2 ± 2.5 , $P=0.038$, Fig. 4A). As for extent of lesion involvement, $\text{SUR}_{\text{Liver}}$ and $\text{SUR}_{\text{Blood}}$ in disseminated disease were significantly higher than those in localized pulmonary disease (median $\text{SUR}_{\text{Liver}}$, 3.8 ± 1.6 vs. 1.9 ± 1.1 , $P=0.016$, Fig. 4B; median $\text{SUR}_{\text{Blood}}$, 5.5 ± 2.6 vs. 2.7 ± 1.8 , $P=0.026$, Fig. 4C). As for the severity of NTM-PD, the median $\text{SUV}_{\text{Marrow}}$ and $\text{SUV}_{\text{I-Lung}}$ in patients with severe NTM-PD were significantly higher than those in patients with non-severe NTM-PD (median $\text{SUV}_{\text{Marrow}}$, 4.4 ± 2.0 vs. 2.4 ± 0.8 , $P=0.027$, Fig. 4D; median $\text{SUV}_{\text{I-Lung}}$, 7.7 ± 4.3 vs. 4.3 ± 2.3 , $P=0.036$). There were no significant differences in the metabolic parameters of MLV and TLG between the localized pulmonary disease group and the disseminated disease group, the severe and non-severe NTM-PD group, and the immunocompetent and immunocompromised patients.

Receiver operating characteristic (ROC) curves were drawn to evaluate the consistency between the ^{18}F -FDG PET/CT metabolic parameters and clinical features (Fig. 4). The area under the curve (AUC) values in immunocompromised and immunocompetent groups were 0.794 for SUV_{Top} ($P=0.02$) (Fig. 4G). The cut-off value of SUV_{Top} was 7.1, and the sensitivity and specificity of ^{18}F -FDG PET/CT for immunocompromised states in NTM patients were 88.9% and 64.3%, respectively. The AUC in group of the localized pulmonary NTM infection and the disseminated NTM infection group were 0.819 for $\text{SUR}_{\text{Liver}}$ ($P=0.023$) and 0.814 for $\text{SUR}_{\text{Blood}}$ ($P=0.025$) (Fig. 4I). When the cut-off values of $\text{SUR}_{\text{Liver}}$ and $\text{SUR}_{\text{Blood}}$

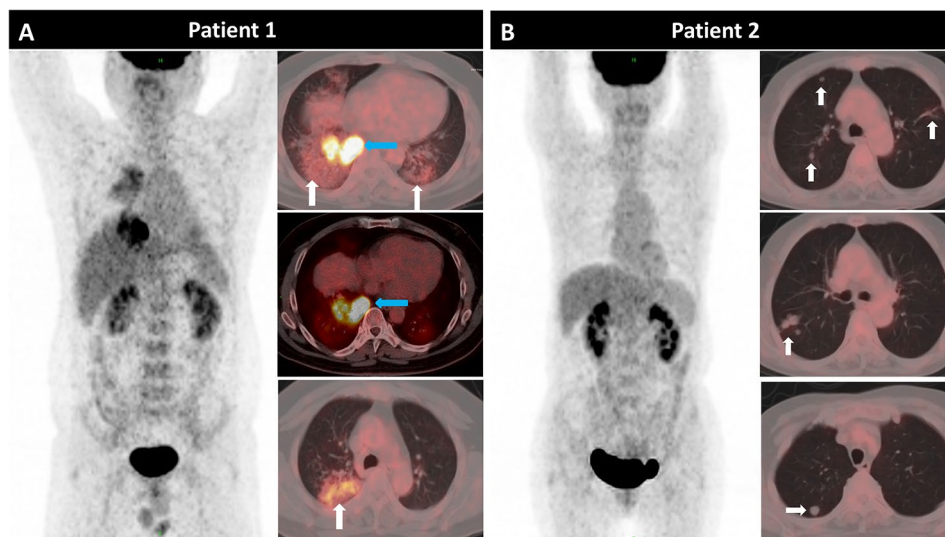


Fig. 2 Patient 1 (No.1): A 38-year-old male patient presented with cough, phlegm and intermittent fever for two months. The pathology of the pulmonary puncture suggested chronic granulomatous inflammation of the lungs. Finally, metagenomics next-generation sequencing (mNGS) of alveolar lavage fluid confirmed *M. abscessus* infection. Multiple patchy shadows (white arrows, $SUV_{max} = 11.3$) and consolidation (blue arrows, $SUV_{max} = 3.7$) in both lungs on the axial slices of ^{18}F -FDG PET/CT scan images. Patient 2 (No.10): A 60-year-old female patient with a history of acute lymphocyte leukemia. After one cycle of chemotherapy, opportunistic intracellular mycobacterial infection appeared in both lungs and was confirmed by TB-DNA-PCR of the sputum. The patient was given active anti-infection treatment (oral azithromycin + ethambutol + rifampicin for 5 months). To assess the tumor activity after treatment, an ^{18}F -FDG PET/CT scan was performed, which revealed multiple FDG-unavid nodules (white arrows, $SUV_{max} = 2.2$) in the right lung. The pathology of the wedge resection of the right lung nodule indicated pulmonary granulomatosis

were 2.8 and 4.4, respectively, the sensitivity and specificity of ^{18}F -FDG PET/CT for disseminated NTM infection were 83.3% and 70.6%, and 83.3% and 52.9%, respectively. The AUC in the severe and non-severe groups were 0.897 for SUV_{Marrow} ($P=0.001$) and 0.688 for SUV_{I-Lung} ($P=0.158$), respectively (Fig. 4H). When the cut-off values of SUV_{Marrow} and SUV_{I-Lung} were 3.1 and 4.6, respectively, the sensitivity and specificity of ^{18}F -FDG PET/CT for the identification severity of NTM-PD were 76.9% and 88.9%, and 76.9% and 55.9%, respectively.

Correlations between the metabolic parameters of ^{18}F -FDG PET/CT and the clinical laboratory results

Spearman's correlation analysis (Fig. 5) revealed a significant positive correlation between serum PCT, IL-6 and SUV_{Marrow} ($r=0.507$ and 0.530 , $p<0.05$). Furthermore, serum PCT and ferritin were significantly positively related to SUV_{Spleen} ($r=0.577$ and 0.558 , respectively, $p<0.05$).

Discussion

Non-tuberculous mycobacteria (NTM) are ubiquitously present in the environment and include opportunistic pathogens that can cause various diseases in multiple organs in both immunocompromised and immunocompetent individuals. Recently, the prevalence of NTM diseases have increased globally, which are now recognized to represent an emerging public health problem [1]. According to established criteria for NTM disease

treatment [10, 11], it strongly recommended that individuals receive a period of longitudinal assessment (including immune status, the severity and risk of progressive NTM infection, and the extent of lesion involvement) before a decision is made to start treatment. Therefore, it is critical to develop noninvasive imaging tools for evaluating active lesions, immune status, and the extent of lesion involvement [12]. Previous studies have revealed the usefulness of ^{18}F -FDG PET in differentiating latent from active TB and evaluating early therapeutic response to anti-TB. Moreover, high FDG-avid lesions in a patient with TB may also reflect a host immune system response that will ultimately prevail [26].

^{18}F -FDG PET/CT has revolutionized oncology care owing to its mechanism of action, including being taken up by cell surface transporters (mainly the glucose transporter-1 and 3, GLUT-1 and 3) and being transformed by the rate-limiting glycolytic enzyme hexokinase into FDG-6-phosphate [13]. Infection and inflammation contribute to enhancing vascular permeability and the release of inflammatory mediator expressing increased levels of GLUT-1 and 3 (macrophages, neutrophils), as well as increased HK activity, resulting in greater ^{18}F -FDG delivery to affected sites [13]. Furthermore, ^{18}F -FDG PET/CT has been used for diagnosing tumor, infection, fever of unknown origin and assessing therapy response due to a whole-body imaging and changes in FDG metabolic parameters ahead of morphological changes by conventional imaging techniques (CT and MRI). Therefore,

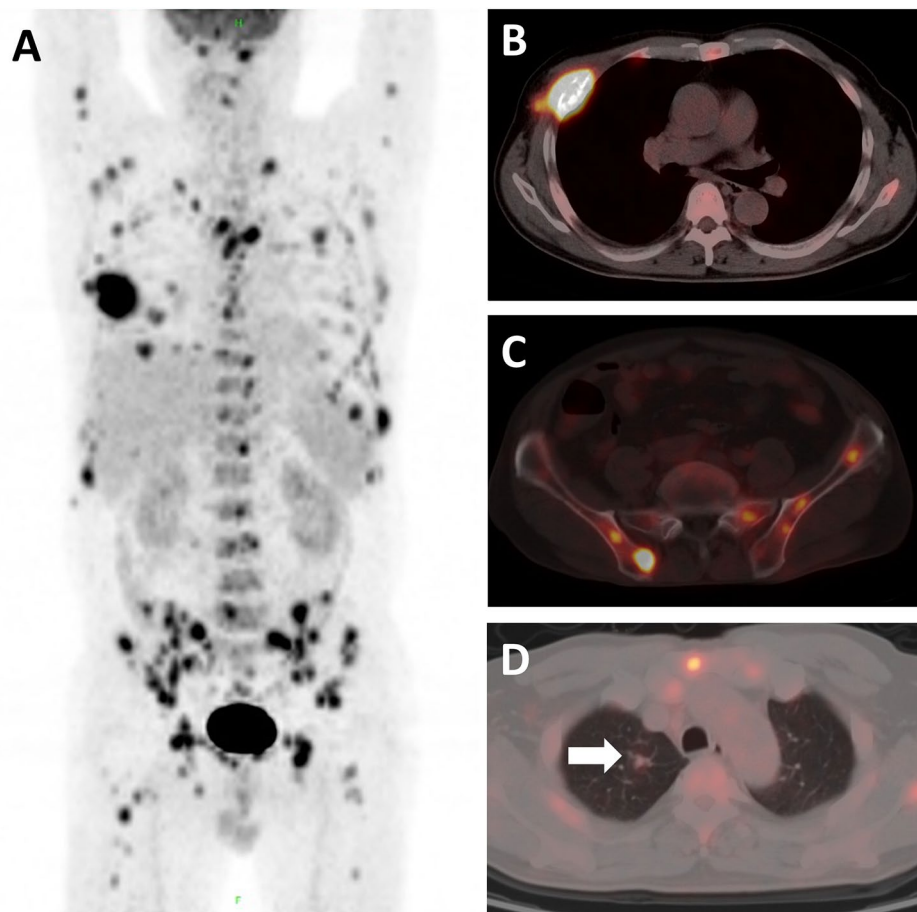


Fig. 3 A 47-year-old man (No.2) presented with right calf and chest pain, fever, and sweating for one month. Laboratory examination revealed significant increases in leukocyte count ($19 \times 10^9/L$), erythrocyte sedimentation rate (77 mm/hour), and C-reactive protein level (87 mg/L). ^{18}F -FDG PET/CT showed diffuse bony destruction with increased high FDG uptake ($SUV_{max} = 14.8$) and mild-uptake small nodule in the upper lobe of the right lung (white arrows, $SUV_{max} = 2.0$). Finally, *M. intracellulare* was confirmed by sputum culture of a rib lesion after removal in orthopedics

^{18}F -FDG PET/CT has been widely used not only for the diagnosis of infectious and inflammatory diseases but also in the evaluation active stage of systemic disease [13]. SUV_{max} and SUR are the most commonly used imaging biomarkers to assess FDG uptake levels. Besson FL et al. [27] indicated that there was a significant improvement in specificity by using $SUR_{Liver} > 1$ compared to visual analysis. In the present study, we collected ^{18}F -FDG PET/CT scanning data from 22 patients with NTM-PD with a median SUV_{max} of 6.6 (range: 1.2–13.9), which was higher than that reported previously (median SUV_{max} of 4.2) [28]. It may possible be more patients with disseminated NTM (17/23) in our study. Moreover, ^{18}F -FDG PET/CT showed an intense or moderate ^{18}F -FDG uptake in both intra-pulmonary and extra-pulmonary lesions in 21 patients, and high FDG-uptake ($SUV_{max} > 2.5$) was observed in 19 patients with intra-pulmonary lesions and 15 patients with extra-pulmonary lesions, suggesting an active stage of the disease. Sinner V et al. [29] reported that the activity of the chorioretinal lesions with NTM infection corresponded to disease progression. The above

evidences highlight that ^{18}F -FDG PET/CT can be of great value to assess the extent of active NTM lesion, particularly for extra-pulmonary lesions, since obtaining tissue or fluid for culture or mNGS may be not always possible or too invasive.

NTM are opportunistic pathogens to humans. Exposure to NTM organisms in the environment in common in day-to-day life, while NTM diseases occur infrequently due to their lower virulence than *Mycobacterium tuberculosis*. However, to date, it has become apparent that some individuals are prone to NTM diseases, particularly immunosuppressed patients with reduced cell-mediated immunity [3–5]. The rate of glucose utilization is accentuated by immune cell activation during inflammation and infection. ^{18}F -FDG PET/CT has provided the most robust evidence regarding this phenomenon in the initial and treatment response assessment of IFD (invasive fungal disease) in immunocompromised patients [30]. The cases selected for our study included 9 (39.1%) immunosuppressed patients and 14 (60.9%) immunocompetent patients. SUV_{Top} in immunocompetent patients was

Table 3 Comparison of clinical and ¹⁸F-FDG PET/CT characteristics among groups with different immune status, extent of lesion involvement and severity of NTM-PD

Characteristics	Immune status			Extent of lesion involvement			Severity of NTM-PD		
	Immunocompromised	Immunocompetent	P	Localized	Disseminated	P	Severe	Non-severe	P
White cell count($\times 10^9/L$)	6.2 \pm 4.3	10.1 \pm 4.8	0.062	8.4 \pm 4.1	8.6 \pm 5.3	0.882	9.4 \pm 5.6	7.4 \pm 3.5	0.354
Neutrophilic granulocyte count ($\times 10^9/L$)	4.2 \pm 3.8	7.9 \pm 4.9	0.068	5.7 \pm 4.1	6.8 \pm 5.1	0.642	7.2 \pm 5.6	5.3 \pm 2.8	0.378
lymphocyte count($\times 10^9/L$)	1.3 \pm 1.2	1.4 \pm 0.9	0.807	1.5 \pm 1.4	1.3 \pm 0.9	0.620	1.5 \pm 1.2	1.1 \pm 0.5	0.357
Red blood cell count($\times 10^9/L$)	3.5 \pm 1.0	3.9 \pm 0.7	0.184	3.9 \pm 0.8	3.7 \pm 0.8	0.685	3.7 \pm 1.0	3.8 \pm 0.5	0.945
Hemoglobin (g/dl)	102.7 \pm 32.3	112.7 \pm 22.7	0.386	117.7 \pm 25.2	104.9 \pm 7.1	0.301	107.0 \pm 30.4	111.7 \pm 20.9	0.692
Platelet count ($\times 10^9/L$)	240.0 \pm 104.7	284.7 \pm 126.3	0.386	225.4 \pm 115.6	285.4 \pm 117.9	0.272	314.0 \pm 119.3	194.3 \pm 73.1	0.003*
C-reactive protein (mg/L)	37.2 \pm 36.1	64.3 \pm 64.8	0.271	19.0 \pm 10.1	64.9 \pm 60.4	0.066	56.3 \pm 55.1	42.5 \pm 56.7	0.569
Erythrocyte sedimentation rate (mm/H)	46.7 \pm 33.6	43.5 \pm 35.8	0.879	27.6 \pm 15.3	36.6 \pm 34.9	0.220	40.7 \pm 38.7	10.6 \pm 16.2	0.040
The percentage of total T lymphocyte (%)	766.0 \pm 726.7	1032.2 \pm 444.2	0.494	60.9 \pm 28.6	63.8 \pm 27.9	0.880	69.6 \pm 23.3	51.6 \pm 31.8	0.305
IL-6 (pg/ml)	35.6 \pm 57.5	23.6 \pm 44.7	0.579	36.3 \pm 65.8	24.7 \pm 42.1	0.615	39.9 \pm 60.8	10.2 \pm 7.1	0.163
TNF- α (pg/ml)	11.8 \pm 24.2	3.0 \pm 2.1	0.127	10.6 \pm 2.6	21.8 \pm 2.1	0.221	21.1 \pm 2.5	9.4 \pm 3.1	0.341
Lactate dehydrogenase (U/L)	218.8 \pm 52.6	196.4 \pm 66.3	0.404	214.9 \pm 55.9	200.0 \pm 64.5	0.626	217.6 \pm 68.4	185.9 \pm 44.3	0.233
SUV _{I-lung}	5.5 \pm 3.9	7.2 \pm 3.9	0.338	5.15 \pm 3.55	6.7 \pm 4.3	0.437	7.7 \pm 4.3	4.3 \pm 2.7	0.036*
SUV _{E-lung}	5.2 \pm 2.8	6.9 \pm 7.5	0.606	NA [#]	NA	NA	8.5 \pm 7.4	4.5 \pm 2.1	0.214
SUV _{Top}	5.2 \pm 2.5	10.0 \pm 6.4	0.038*	5.6 \pm 3.6	9.3 \pm 6.1	0.153	9.0 \pm 3.7	7.5 \pm 7.1	0.559
SUR _{Liver}	2.7 \pm 1.4	4.3 \pm 0.25	0.095	1.9 \pm 1.1	3.8 \pm 1.6	0.016*	3.4 \pm 1.2	2.8 \pm 2.3	0.464
SUR _{Blood}	4.7 \pm 2.9	6.6 \pm 4.3	0.258	2.7 \pm 1.8	5.5 \pm 2.6	0.026*	5.3 \pm 2.1	4.3 \pm 3.3	0.410
SUV _{Liver}	2.6 \pm 0.6	2.7 \pm 0.7	0.825	2.7 \pm 0.4	2.6 \pm 0.7	0.762	2.7 \pm 0.6	2.6 \pm 0.6	0.586
SUV _{Marrow}	3.6 \pm 1.6	3.7 \pm 2.3	0.896	3.0 \pm 0.08	3.9 \pm 2.3	0.320	4.4 \pm 2.0	2.4 \pm 0.8	0.027*
SUV _{Spleen}	2.7 \pm 1.4	2.4 \pm 0.4	0.444	2.0 \pm 1.0	2.4 \pm 1.3	0.489	2.5 \pm 1.3	1.8 \pm 0.7	0.131
MLV(cm ³)	56.4 \pm 50.2	172.6 \pm 261.9	0.206	35.6 \pm 59.0	160.1 \pm 245.0	0.204	116.2 \pm 135.9	127.7 \pm 271.5	0.900
TLG(ml*SUV)	237.1 \pm 256.8	748.3 \pm 1230.9	0.236	119.7 \pm 210.9	705.1 \pm 1149.9	0.201	465.9 \pm 559.1	582.9 \pm 1299.1	0.785

¹⁸F-FDG PET/CT: ¹⁸F-fluorodeoxyglucose positron emission tomography/computed tomography; NTM: Non-tuberculous mycobacterial infection; NTM-PD: Non-tuberculous mycobacterial pulmonary diseases; SUV_{Top}: The most FDG-avid lesion in the whole body; SUV_{I-lung}: SUV_{max} of lung lesions, SUV_{E-lung}: SUV_{max} of extra-lung lesions; SUV_{Liver}: SUV_{max} of liver; SUV_{Spleen}: SUV_{max} of spleen; SUV_{Marrow}: SUV_{max} of marrow; SUR_{Liver}: SUV_{max} ratio of lesion-to-liver; SUR_{Blood}: SUV_{max} ratio of lesion-to-blood pool. MLV: the metabolic lesion volume; TLG: total lesion glycolysis

NA[#]: Localized groups were defined as NTM patients with only pulmonary involvement

*: P value less than 0.05 was considered statistically significant

significantly higher than that in immunocompromised patients. Moreover, the cut-off value of SUV_{Top} was 7.1, and the sensitivity and specificity of ¹⁸F-FDG PET/CT for compromised immune status in NTM patients were 88.9% and 64.3%, respectively. These results indicated that SUV_{Top} was significantly positively related to immune cell activation due to the upregulation of GLUT-1 and 3, along with increased hexokinase activity [13], whereas immunosuppressed patients exhibit the disruption or depletion of cell-mediated immunity and immune cell activation in immunocompromised patients

is lower than that in immunocompetent patients. NTM guidelines [10, 11] strongly recommend that immunocompromised patients with NTM infection require a longer duration and dose of treatment. In future work, we aim to expand the sample size and conduct prospective experiments to further explore the relationship of immune function and metabolic parameters of FDG PET/CT in NTM patients.

NTM can affect any organ in the body, and the main clinical manifestations in adults are localized NTM pulmonary disease and/or other disseminated diseases.

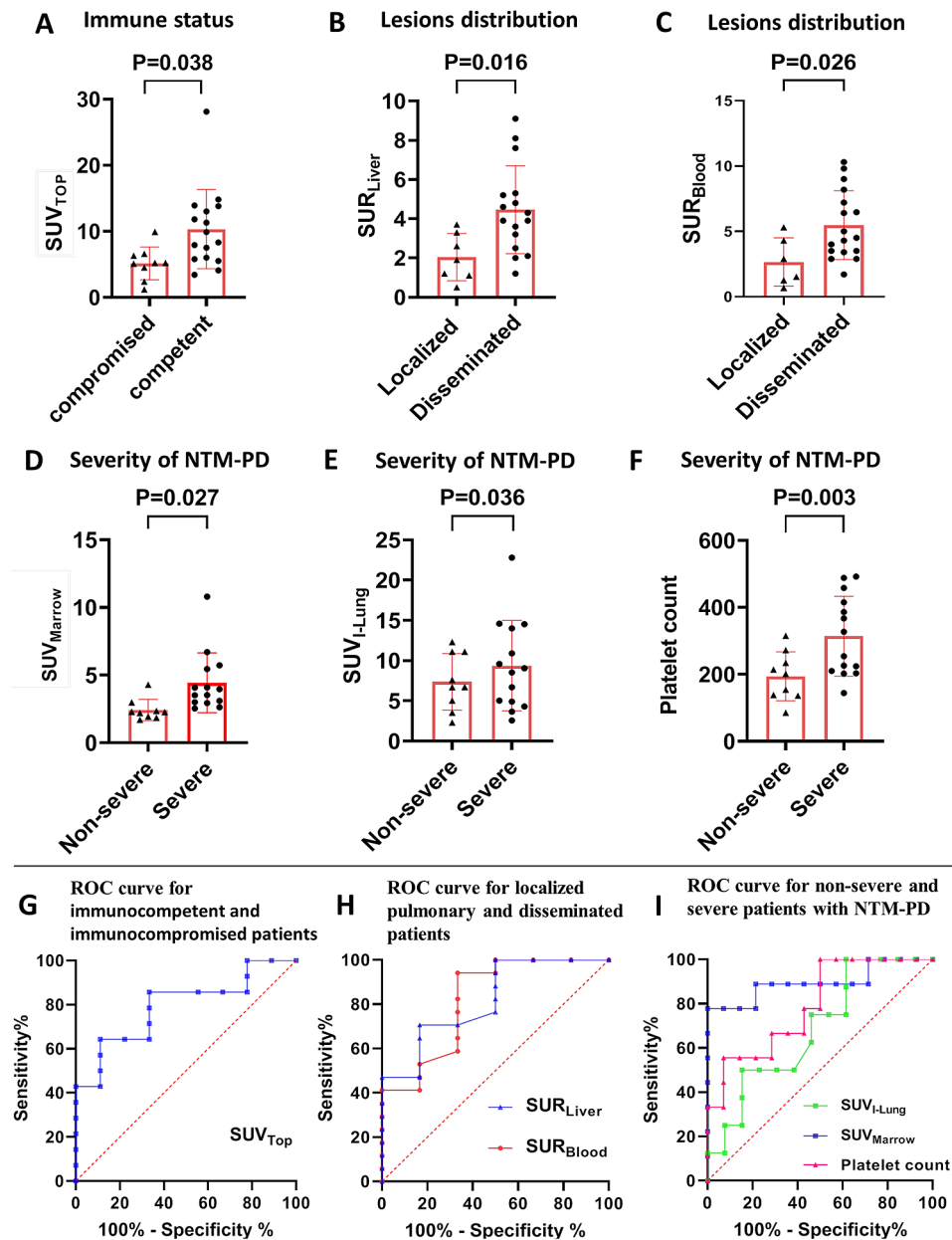


Fig. 4 (A). Comparison of SUV_{TOP} between immunocompromised and immunocompetent patients. (B). Comparison of SUR_{Liver} between the localized pulmonary diseases group and the disseminated diseases group. (C). Comparison of SUR_{Blood} between the localized pulmonary diseases group and the disseminated diseases group. (D). Comparison of SUV_{Marrow} between severe NTM-PD and non-severe NTM-PD. (E). Comparison of SUV_{I-Lung} between severe NTM-PD and non-severe NTM-PD. (F). Comparison of platelet count between severe NTM-PD and non-severe NTM-PD. (G). ROC curve analysis for predicting immunocompromised status in NTM patients using SUV_{TOP} values of ¹⁸F-FDG-PET/CT scans. (H). ROC curve analysis for predicting disseminated NTM infection using SUR_{Liver} and SUR_{Blood} values of ¹⁸F-FDG-PET/CT scans. (I). Receiver operating characteristic curve (ROC) analysis for predicting severe NTM-PD using platelet count, and SUV_{Marrow}, and SUV_{I-Lung} values of ¹⁸F-FDG-PET/CT scans

Disseminated NTM diseases (defined as the involvement of two or more non-contiguous body organs) often occur in patients with an immune defect, and 2–8 per cent of patients with disseminated diseases may have concurrent pulmonary involvement [5]. The *Mycobacterium avium* complex (MAC) and rapidly growing mycobacteria (RGM) have been identified as important pathogens contributing disseminated diseases [31]. Thus, early

diagnosis and treatment is essential to minimize morbidity and costs, as well as prevent long-term disability [5]. In this study, extra-pulmonary lesions with abnormally high ¹⁸F-FDG FDG uptake were found in 17 patients (73.8%) with disseminated diseases. In these patients, ¹⁸F-FDG PET/CT showed increased ¹⁸F-FDG accumulation in the lymph node (14 cases), bone (6 cases), subcutaneous tissue (1 case), spleen (1 case), and adrenal gland

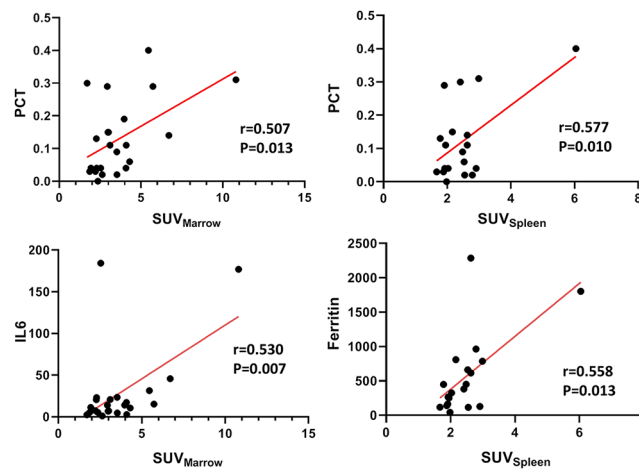


Fig. 5 Spearman's rank analysis of ^{18}F -FDG uptake ($\text{SUV}_{\text{Spleen}}$ and $\text{SUV}_{\text{Marrow}}$) and laboratory markers such as interleukin 6 (IL-6), procalcitonin (PCT) and ferritin

(1 case). The metabolic parameters $\text{SUR}_{\text{Liver}}$ and $\text{SUR}_{\text{Blood}}$ in disseminated diseases were significantly higher than those in localized pulmonary diseases. When the cut-off values of $\text{SUR}_{\text{Liver}}$ and $\text{SUR}_{\text{Blood}}$ were 2.8 and 4.4, respectively, the sensitivity and specificity of ^{18}F -FDG PET/CT for disseminated diseases were 83.3% and 70.6%, and 83.3% and 52.9%, respectively. These results showed that an active NTM lesion readily takes up ^{18}F -FDG, both in pulmonary and extra-pulmonary lesions. Moreover, NTM patients with high $\text{SUR}_{\text{Liver}}$ and $\text{SUR}_{\text{Blood}}$ level were related to disseminated diseases. This result needs to be confirmed in the next prospective study.

According to the guidelines for the management of non-tuberculosis mycobacterial pulmonary disease by the British Thoracic Society [11], as the treatment of NTM pulmonary disease is arduous, lengthy and costly, several factors should be considered before a decision is made to begin treatment, such as the severity of NTM-PD, the risk of progressive NTM-PD, the presence of any comorbidities, and the goals of treatment [9, 12]. ^{18}F -FDG PET/CT is a functional imaging technique that detects metabolically active areas by measuring the accumulation of ^{18}F -FDG, and may help to establish NTM-PD diagnoses [32]. In the present study, when the cut-off values of $\text{SUV}_{\text{Marrow}}$ and $\text{SUV}_{\text{I-Lung}}$ were 3.1 and 4.6, respectively, the sensitivity and specificity of ^{18}F -FDG PET/CT for the identification of NTM-PD severity were 76.9% and 88.9%, and 76.9% and 55.9%, respectively. A high FDG uptake of NTM-PD lesion indicates inflammatory activity, significant mycobacterial pathogenicity, or an elicited systemic response (such as in Patient 1 in Fig. 2), while normal or low FDG uptake shows inflammation regression or scar formation (such as in Patient 2 in Fig. 2). Therefore, the indices $\text{SUV}_{\text{I-Lung}}$ and $\text{SUV}_{\text{Marrow}}$ can both suggest systemic inflammatory response, either directly after NTM infection or indirectly by reflecting

the virulence of the bacteria. NTM-PD patients with $\text{SUV}_{\text{Marrow}} \geq 3.1$ and $\text{SUV}_{\text{I-Lung}} \geq 4.6$ may likely be severe NTM if effective treatment is delayed. Therefore, these metabolic parameters can contribute to the planning of appropriate treatment for NTM. Furthermore, the Spearman's correlation analysis revealed a significant positive correlation between serum IL-6 and $\text{SUV}_{\text{Marrow}}$, ferritin and $\text{SUV}_{\text{Spleen}}$. The PET metabolic parameters of bone marrow and spleen may reflect the development and progression of a cytokine storm [33]. To this end, the value of ^{18}F -FDG PET/CT in predicting immune cell activation and evaluating treatment response of NTM patients deserves further investigation.

This study inevitably has some limitations. First, it was conducted at a single center, and the sample size was limited ($n=23$). All images were acquired on the same PET/CT scanner model (Biograph version; Siemens, Germany), imaging protocol, and reconstruction. Second, because this was a retrospective study, the use of ^{18}F -FDG PET/CT in the assessment of patients potentially introduced a bias toward a disseminated NTM infection cohort. Third, in our study, each patient underwent an ^{18}F -FDG PET/CT scan only once (baseline assessment in 16 patients and anti-NTM pre-PET in 7 patients) and lacked post-treatment reassessment. Fourth, 10 patients were misdiagnosed malignancies (multiple myeloma, lung cancer and lymphadenoma, etc.) by ^{18}F -FDG PET/CT (Table 1). So, ^{18}F -FDG PET/CT has a limited role in differentiating disseminated NTM diseases from malignancies. Lastly, metabolic measurements reflected the FDG uptake by inflammatory cells rather than NTM. Thus, NTM-specific radiolabeled compounds and imaging approaches urgently need to be developed. In addition, a multicenter, prospective analysis should be designed in a future study to attain a better representation of NTM-infected patients.

Conclusion

^{18}F -FDG PET/CT is a useful tool in the diagnosis, evaluation of disease activity, immune status, and extent of lesion involvement in NTM patients, and can contribute to planning the appropriate treatment for NTM.

Abbreviations

NTM	Non-tuberculous mycobacteria
NTM-PD	Non-tuberculous mycobacterial pulmonary diseases
MDS	Myelodysplastic syndromes
AIDS	Acquired immunodeficiency syndrome
COPD	Chronic obstructive pulmonary disease
BALF	Bronchoalveolar lavage fluid
NTM-DNA-PCR	PCR assay for non-tuberculous mycobacteria DNA
IIP	Idiopathic interstitial pneumonia
mNGS	Metagenomic next-generation sequencing
^{18}F -FDG PET/CT	^{18}F -fluorodeoxyglucose positron emission tomography/computed tomography
CT	Computed tomography
MRI	Magnetic resonance imaging
SUV_{top}	The most FDG-avid lesion in the whole body
$\text{SUV}_{\text{I-Lung}}$	SUV_{max} of intra-pulmonary lesions
$\text{SUV}_{\text{E-Lung}}$	SUV_{max} of extra-pulmonary lesions
$\text{SUV}_{\text{Liver}}$	SUV_{max} of the liver
$\text{SUV}_{\text{spleen}}$	SUV_{max} of the spleen
$\text{SUV}_{\text{Marrow}}$	SUV_{max} of the marrow
$\text{SUR}_{\text{Liver}}$	$\text{SUV}_{\text{Top}}/\text{SUV}_{\text{max}}$ of the liver ($\text{SUR}_{\text{Liver}}$)
$\text{SUR}_{\text{Blood}}$	$\text{SUV}_{\text{Top}}/\text{SUV}_{\text{max}}$ of the blood ($\text{SUR}_{\text{Blood}}$)
MLV	Metabolic lesion volume
TLG	Total lesion glycolysis
ROC	Receiver operating characteristic curve
AUCs	Areas under the curve

Supplementary Information

The online version contains supplementary material available at <https://doi.org/10.1186/s12931-024-02757-7>.

Supplementary Material 1

Acknowledgements

We gratefully acknowledge our colleagues for their comments on this study.

Author contributions

Authors' contributions DC and XS: Study conception and design; drafting of manuscript; critical revision; review, analysis and interpretation of scientific literature; YC was involved in the management of the specimen samples of the patient; drafting of manuscript; KZ, KL, ZW, SY and GW: Drafting of manuscript; review, analysis and interpretation of scientific literature. All authors have contributed to the manuscript and approved its final version.

Funding

This work was received by grants from the National Natural Science Foundation of China (NSFC) (82071965) and Huadong Medicine Joint Funds of the Zhejiang Provincial Natural Science Foundation of China (LHDMZ22H300010).

Declarations

Informed consent

Written informed consent was not required because of the retrospective nature for this study.

Ethical approval

This retrospective study protocol was reviewed and approved by the Clinical Research Ethics Committee of the First Affiliated Hospital, Zhejiang University School of Medicine (No. IIT20220576A). The requirement for informed consent

was waived by the Clinical Research Ethics Committee of the First Affiliated Hospital, Zhejiang University School of Medicine due to retrospective study.

Conflict of interest

The authors of this manuscript declare no relationships with any companies, whose products or services may be related to the subject matter of the article.

Author details

¹Department of Nuclear Medicine, The First Affiliated Hospital, Zhejiang University School of Medicine, 79 Qingchun Road, Hangzhou 310003, China

²State Key Laboratory for Diagnosis and Treatment of Infectious Diseases, The First Affiliated Hospital, Zhejiang University School of Medicine, Hangzhou 310003, China

Received: 9 November 2023 / Accepted: 4 March 2024

Published online: 18 March 2024

References

- Johansen MD, Herrmann JL, Kremer L, Non-tuberculous mycobacteria and rise Mycobacterium abscessus Nat Rev Microbiol. 2020;18(7):392–407.
- Meoli A, Deolmi M, Iannarella R, Esposito S. Non-Tuberculous Mycobacterial Dis Child Pathogens. 2020;9(7):553–65.
- Zhou L, Xu D, Liu H, Wan K, Wang R, Yang Z. Trends in the prevalence and antibiotic resistance of non-tuberculous mycobacteria in Mainland China, 2000–2019: systematic review and Meta-analysis. Front Public Health. 2020;8:295–304.
- Ahmed I, Tiberi S, Farooqi J, Jabeen K, Yeboah-Manu D, Migliori GB, Hasan R. Non-tuberculous mycobacterial infections-A neglected and emerging problem. Int J Infect Dis. 2020;92S:546–50.
- Sharma SK, Upadhyay V. Epidemiology, diagnosis & treatment of non-tuberculous mycobacterial diseases. Indian J Med Res. 2020;152(3):185–226.
- Ratnatunga CN, Lutzky VP, Kupz A, Doolan DL, Reid DW, Field M, Bell SC, Thomson RM, Miles JJ. The rise of Non-tuberculosis Mycobacterial Lung. Disease Front Immunol. 2020;11:303–15.
- Eisenberg I, Yasin A, Fuks L, Stein N, Saliba W, Kramer MR, Adir Y, Shteinberg M. Radiologic Characteristics Non-tuberculous Mycobact Infect Patients Bronchiectasis Lung. 2020;198(4):715–22.
- Chanda-Kapata P, Kapata N, Klinkenberg E, Mulenga L, Tembo M, Kateman-gwe P, Sunkutu V, Mwaba P, Grobusch MP. Non-tuberculous mycobacteria (NTM) in Zambia: prevalence, clinical, radiological and microbiological characteristics. BMC Infect Dis. 2015;15:500–7.
- Porvaznik I, Solovič I, Mokry J. Non-tuberculous mycobacteria: classification, Diagnostics, and Therapy. Adv Exp Med Biol. 2017;944:19–25.
- Daley CL, Iaccarino JM, Lange C, Cambau E, Wallace RJ Jr, Andrejak C, Böttger EC, Brozek J, Griffith DE, Guglielmetti L, Huitt GA, Knight SL, Leitman P, Marras TK, Olivier KN, Santin M, Stout JE, Tortoli E, van Ingen J, Wagner D, Winthrop KL. Treatment of nontuberculous mycobacterial pulmonary disease: an official ATS/ERS/ESCMID/IDSA clinical practice guideline. Eur Respir J. 2020;56(1):2000535.
- Haworth CS, Banks J, Capstick T, Fisher AJ, Gorsuch T, Laurenson IF, Leitch A, Loebinger MR, Millburn HJ, Nightingale M, Ormerod P, Shingadia D, Smith D, Whitehead N, Wilson R, Floto RA. British Thoracic Society guidelines for the management of non-tuberculous mycobacterial pulmonary disease (NTM-PD). Thorax. 2017;72(Suppl 2):ii1–64.
- Henkle E, Aksamit T, Barker A, Daley CL, Griffith D, Leitman P, Leitman A, Malanga E, Marras TK, Olivier KN, Prevots DR, Prieto D, Quittner AL, Skach W, Walsh JW, Winthrop KL, NTMRC Patient Advisory Panel. Patient-centered Research priorities for Pulmonary Nontuberculous Mycobacteria (NTM) infection. An NTM Research Consortium Workshop Report. Ann Am Thorac Soc. 2016;13(9):S379–84.
- Mochizuki T, Tsukamoto E, Kuge Y, Kanegae K, Zhao S, Hikosaka K, Hosokawa M, Kohanawa M, Tamaki N. FDG uptake and glucose transporter subtype expressions in experimental tumor and inflammation models. J Nucl Med. 2001 Oct;42(10):1551–5.
- Vaidyanathan S, Patel CN, Scarsbrook AF, Chowdhury FU. FDG PET/CT in infection and inflammation—current and emerging clinical applications. Clin Radiol. 2015;70(7):787–800.

15. O'Brien DP, Currie BJ, Krause VL. Nontuberculous mycobacterial disease in northern Australia: a case series and review of the literature. *Clin Infect Dis*. 2000;31(4):958–67.
16. Polverosi R, Guarise A, Balestro E, Carloni A, Dalpiaz G, Feragalli B. High-resolution CT of nontuberculous mycobacteria pulmonary infection in immunocompetent, non-HIV-positive patients. *Radiol Med*. 2010;115(2):191–204.
17. Sathekge M, Maes A, D'Asseler Y, Vorster M, Gongxeka H, Van de Wiele C. Tuberculous lymphadenitis: FDG PET and CT findings in responsive and nonresponsive disease. *Eur J Nucl Med Mol Imaging*. 2012;39:1184–90.
18. Kim IJ, Lee JS, Kim SJ, Kim YK, Jeong YJ, Jun S, Nam HY, Kim JS. Double-phase 18F-FDG PET-CT for determination of pulmonary tuberculoma activity. *Eur J Nucl Med Mol Imaging*. 2008;35(4):808–14.
19. Namkoong H, Fujiwara H, Ishii M, Yagi K, Haraguchi M, Matsusaka M, Suzuki S, Asakura T, Asami T, Saito F, Fukunaga K, Tasaka S, Betsuyaku T, Hasegawa N. Immune reconstitution inflammatory syndrome due to *Mycobacterium avium* complex successfully followed up using 18 F-fluorodeoxyglucose positron emission tomography-computed tomography in a patient with human immunodeficiency virus infection: a case report. *BMC Med Imaging*. 2015;15:24.
20. Lin KH, Wang JH, Peng NJ. Disseminated nontuberculous mycobacterial infection mimic metastases on PET/CT scan. *Clin Nucl Med*. 2008;33(4):276–7.
21. Ishii T, Tamura A, Matsui H, Nagai H, Akagawa S, Hebisawa A, Ohta K. Disseminated *Mycobacterium avium* complex infection in a patient carrying autoantibody to interferon- γ . *J Infect Chemother*. 2013;19(6):1152–7.
22. Tanaka S, Hoshino Y, Sakagami T, Fukano H, Matsui Y, Hiranuma O. Pathogenicity of *Mycobacterium Phlei*, a non-pathogenic nontuberculous mycobacterium in an immunocompetent host carrying anti-interferon gamma autoantibodies: a case report. *BMC Infect Dis*.
23. Ramirez JA, Musher DM, Evans SE, Dela Cruz C, Crothers KA, Hage CA et al. Treatment of Community-Acquired Pneumonia in Immunocompromised Adults: A Consensus Statement Regarding Initial Strategies. *Chest*. 2020, 158: 1896–1911.
24. Sesin GP, Manzi SF, Pacheco R. New trends in the drug therapy of localized and disseminated *Mycobacterium avium* complex infection. *Am J Health Syst Pharm*. 1996;53(21):2585–90.
25. Ricotta EE, Adjemian J, Blakney RA, Lai YL, Kadri SS, Prevots DR. Extrapulmonary Nontuberculous Mycobacteria infections in hospitalized patients, United States, 2009–2014. *Emerg Infect Dis*. 2021;27(3):845–52.
26. Ankras AO, van der Werf TS, de Vries EF, Dierckx RA, Sathekge MM, Glaudemans AW. PET/CT imaging of *Mycobacterium tuberculosis* infection. *Clin Transl Imaging*. 2016;4:131–44.
27. Besson FL, Parienti JJ, Biennu B, Prior JO, Costo S, Bouvard G, Agostini D. Diagnostic performance of ^{18}F -fluorodeoxyglucose positron emission tomography in giant cell arteritis: a systematic review and meta-analysis. *Eur J Nucl Med Mol Imaging*. 2011;38(9):1764–72.
28. Stroffolini G, Gaviraghi A, Penna D, Piccioni P, Venuti F, Botto C, Trezzi M, Betti M, Sestini S, Erba PA, Lupia T, Di Perri G, Aliberti S, Calcagno A. 18-fluorodeoxyglucose positron emission tomography (FDG-PET) in patients with non-tuberculous mycobacterial infections. *J Infect*. 2023;87(5):462–4.
29. Sinner V, Rüesch R, Valmaggia C, Todorova M. Choroidal manifestation of systemic non-tuberculous mycobacterial infection: a Case Series. *Klin Monbl Augenheilkd*. 2020;237(4):493–6.
30. Lawal IO, Mokoala KMG, Kgatle MM, Dierckx RAJO, Glaudemans AWJM, Sathekge MM, Ankras AO. Radionuclide Imaging of Invasive Fungal Disease in Immunocompromised Hosts. *Diagnostics (Basel)*. 2021;11(11):2057.
31. Henkle E, Winthrop KL. Nontuberculous mycobacteria infections in immunosuppressed hosts. *Clin Chest Med*. 2015;36(1):91–9.
32. Del Giudice G, Bianco A, Cennamo A, Santoro G, Bifulco M, Marzo C, Mazarella G. Lung and nodal involvement in Nontuberculous Mycobacterial Disease: PET/CT role. *Biomed Res Int*. 2015;2015:353202.
33. Signore A, Lauri C, Bianchi MP, et al. [^{18}F]FDG PET/CT in patients affected by SARS-CoV-2 and Lymphoproliferative Disorders and treated with Tocilizumab. *J Personalized Med*. 2022;12(11):1839.

Publisher's Note

Springer Nature remains neutral with regard to jurisdictional claims in published maps and institutional affiliations.